Int. J. Morphol.,
43(6):2001-2014, 2025.

Lycium barbarum Polysaccharide Improves Obesity-Induced Muscle Atrophy via Activation of PI3K/AKT Pathway

El Polisacárido de *Lycium barbarum* Mejora la Atrofia Muscular Inducida por la Obesidad Mediante la Activación de la Vía PI3K/AKT

Fan Gong[1,2,3,4]; Yanru Ren[5]; Tingting Cao[3]; Yu Xu[3]; Kun Wang[3]; Jiarui Li[3]; Ze Jin[6]; Anle Wang[7]; Jianning Li[3]; Yi Yang[1,2,3] & Yanhong Wei[1,2,3]

GONG, F.; REN, Y.; CAO, T.; XU, Y.; WANG, K.; LI, J.: JIN, Z.; WANG, A.; LI, J.; YANG, Y. & WEI, Y. *Lycium barbarum* polysaccharide improves obesity-induced muscle atrophy via activation of PI3K/AKT pathway. *Int. J. Morphol., 43(6)*:2001-2014, 2025.

SUMMARY: Abnormal or excessive fat accumulation caused by a sedentary lifestyle and a high-fat diet (HFD) can lead to a loss of muscle mass and strength, ultimately resulting in sarcopenia, a condition known as sarcopenic obesity (SO). This study aimed to investigate the effects of *Lycium barbarum* polysaccharide (LBP) on SO and to explore the underlying mechanisms in order to evaluate its potential as a natural therapeutic agent. Male C57BL/6J mice were fed an HFD for 17 weeks, with LBP administration beginning after 8 weeks and continuing for 9 weeks. Body weight was measured twice weekly. Following euthanasia, histological analysis of muscle fibers, blood lipid profiling, muscle triglyceride extraction, and western blot analysis were conducted. *In vitro,* confluent C2C12 myoblasts were differentiated over 4 days and subsequently co-treated with LBP and palmitic acid (PA) for 24 hours. Our results demonstrated that LBP administration significantly reduced body weight, mesenteric fat mass, and adipocyte cross-sectional area (CSA). Concurrently, LBP increased muscle weight and muscle fiber CSA while decreasing the expression of atrophy-related markers, including muscle atrophy F-box protein (Atrogin-1) and muscle RING-finger protein 1 (MuRF1). Furthermore, LBP improved glucose tolerance and insulin sensitivity by modulating the phosphatidylinositol-3-kinase (PI3K)/protein kinase B (AKT) signaling pathway, which also mitigated excessive lipid accumulation and ectopic fat deposition in skeletal muscle. Activation of the PI3K/AKT pathway by LBP enhanced muscle protein synthesis through increased phosphorylation of p70 ribosomal protein S6 kinase and inhibition of glycogen synthase kinase 3β, while simultaneously suppressing muscle protein degradation by downregulating the expression of Atrogin-1, MuRF1, myostatin, activin A receptor type II B (ActRIIB), and Smad2/3. These findings suggest that LBP is a promising natural agent for the prevention and treatment of SO, exerting its protective effects by correcting glucolipid metabolic disorders and restoring the balance between protein synthesis and degradation in skeletal muscle via the reactivation of the impaired PI3K/AKT pathway.

KEY WORDS: High-fat diet; Sarcopenic obesity; *Lycium barbarum* polysaccharide; PI3K/AKT pathway; Glucolipid metabolism.

[1] Ningxia Regional Key Laboratory of Integrated Traditional Chinese and Western Medicine for Prevention and Treatment of Regional High Incidence Disease, Ningxia Medical University, Yinchuan, China.
[2] Key Laboratory of Hui Ethnic Medicine Modernization, Ministry of Education Ningxia Medical University, Ningxia Medical University, Yinchuan, China.
[3] School of Basic Medicine, Ningxia Medical University, Yinchuan, China.
[4] Department of Orthopedics, People's Hospital of Ningxia Hui Autonomous Region (Ningxia Medical University Affiliated Autonomous Region People's Hospital), Yinchuan, China.
[5] Department of Endocrinology, General Hospital of Ningxia Medical University, Yinchuan, China.
[6] The Third Clinical Medical College of Ningxia Medical University, Yinchuan, China.
[7] The Second Clinical Medical College of Ningxia Medical University, Yinchuan, China.
Fan Gon and Yanru Ren contributed equally to this work.
FUNDING. This work was supported by the National Natural Science Foundation of China (No. 82160171, 82460162), the special talents program of Ningxia Province, China (No. 2024BEH04006). Natural Science Foundation of Ningxia Province, China (2023AAC02038, 2024AAC03264, 2024AAC03233), Key research and development program of Ningxia Province, China (No. 2023BEG02020), and key project of Ningxia Medical University, China (No. XZ2025006).

Received: 2025-08-19 Accepted: 2025-10-07

Abbreviations. The following abbreviations are used in this manuscript:

LBP	*Lycium barbarum* polysaccharide
HFD	High-fat diet
SO	Sarcopenic obesity
CSA	Cross-sectional area
MuRF1	Muscle RING-finger protein 1
Atrogin-1	Muscle atrophy F-box protein
PI3K	Phosphatidylinositol-3-kinase
AKT	Protein kinase B
ActRIIB	Activin A receptor type II B
IGF-1	Insulin-like growth factor-1
IRS-1	Insulin receptor substrate 1
GLUT4	Glucose transporter type 4
GSK3	Glycogen synthase kinase 3
AST	Aspartate aminotransferase
ALT	Alanine transaminase
TC	Total cholesterol
TG	Triglyceride
HDL-C	High-density lipoprotein
LDL-C	Low-density lipoprotein
HOMA-IR	Insulin resistance index

INTRODUCTION

The prevalence of obesity is increasing worldwide, amplifying concerns over the health risks associated with this worsening problem. Sarcopenic obesity (SO), a condition characterized by the coexistence of sarcopenia and obesity, leads to diminished exercise capacity and is often accompanied by increased disability and frailty (Wei *et al*., 2023). Long-term consumption of a high-fat diet (HFD), coupled with a sedentary lifestyle, has emerged as a critical driver of the obesity epidemic. Notably, excessive intake of saturated fats contributes not only to fat mass accumulation but also to elevated comorbidity factors, including glucose intolerance, hyperlipidemia, increased proinflammatory cytokine expression, and insulin resistance in skeletal muscle, which collectively exacerbate sarcopenia (Alalwan, 2020). Given that sarcopenic obesity exerts a more profound impact on metabolic diseases and cardiovascular disease-related mortality compared to either sarcopenia or obesity alone (Roh & Choi, 2020), further exploration of its molecular mechanisms and effective therapeutic strategies is imperative for improving prevention and treatment of this complex condition.

Obesity is a primary cause of muscle atrophy and accelerates the loss of skeletal muscle mass, as skeletal muscle serves as a critical site for glucose uptake and storage. Under normal physiological conditions, insulin facilitates cell growth and differentiation, stimulates protein synthesis and inhibits protein proteolysis (Jun *et al*., 2023). In obesity, the ectopic accumulation of lipids within muscle fibers disrupts insulin signaling and impairs glucose metabolism, thereby inducing skeletal muscle insulin resistance. Insulin resistance can trigger enhanced muscle protein degradation (Han & Choung, 2022). As obesity progresses, adipose tissue loses its ability to store lipids, causing increased serum lipid levels and excessive lipid flux into skeletal muscle. This results in the ectopic accumulation of lipids and their metabolites within muscle fibers. Intramyocellular lipids promote muscle wasting by stimulating inflammation and lipotoxicity, which increase protein degradation and inhibit muscle regeneration (Li *et al*., 2022). Especially, the lipids accumulated in skeletal muscle disrupt insulin signaling, exacerbating muscle atrophy and insulin resistance (Armandi *et al*., 2021).

Sarcopenia, or skeletal muscle atrophy, refers to a reduction in both muscle mass and muscle function. Muscle mass is determined by the balance between protein synthesis and degradation. Insulin-like growth factor-1 (IGF-1) is a key growth factor that regulates both anabolic and catabolic pathways in skeletal muscle. IGF-1 increases skeletal muscle protein synthesis via phosphatidylinositol-3-kinase (PI3K)/ protein kinase B (AKT) pathway (Yoshida & Delafontaine, 2020). In skeletal muscle, insulin binds to and activates the insulin receptor tyrosine kinase, leading to the subsequent phosphorylation of insulin receptor substrate 1 (IRS-1) and activation of the PI3K/AKT pathway. This process promotes translocation of glucose transporter type 4 (GLUT4) to the plasma membrane, facilitating glucose uptake into the skeletal muscle (Deshmukh, 2016). Previous studies have shown that the inhibition of IR, IRS-1, PI3K, AKT and GLUT-4 mRNA expression in rat skeletal muscle leads to skeletal muscle insulin resistance and eventually progresses to type 2 diabetes (Jayaraman *et al*., 2023). When the PI3K/AKT signaling pathway is activated, protein synthesis is enhanced by activating the mammalian target of rapamycin (mTOR) and inactivating glycogen synthase kinase 3 (GSK3) (Rommel *et al*., 2001). PI3K/AKT pathway can also inhibit FoxOs and suppress transcription of E3 ubiquitin ligases that regulate ubiquitin proteasome system (UPS)-mediated protein degradation (Sartori *et al*., 2021). However, in the case of obesity, elevated intramyocellular lipids, stored in skeletal muscle cells, activate serine residues on IRS, leading to the decomposition of IRS and inhibition of PI3K/AKT pathway activation (Han & Choung, 2022; Savova *et al*., 2023; Li *et al*., 2015). This results in exacerbated insulin resistance and muscle atrophy.

Lycium barbarum, a small red berry commonly used for home cooking in China, also is a Chinese traditional herbal medicine. According to the "Ben Cao Gang Mu (Compendium of Materia Medica)", the fruits of *L. barbarum* are said to "strengthens muscles and bones, and exhibit anti-fatigue and anti-aging effects." Previous studies have reported that *L. barbarum* extract increases the number of muscle satellite cells in both adult and aging mice (Meng *et al*., 2023), significantly increases the muscle-to-weight ratio of the tibialis anterior and gastrocnemius muscles in mice, decreases fat content, and enhances muscle endurance (Meng *et al*., 2020). Since we have already confirmed that *L. barbarum* polysaccharide (LBP), the extract of *L. barbarum* berry, has anti- muscle atrophy efficacy against HFD-induced obese rats in a previously study, especially, repairing the mitochondrial structure and function and markedly alleviates HFD-induced muscle atrophy via activation mitophagy pathway (Ren *et al*., 2025). LBP also ameliorates dyslipidemia and insulin resistance (Yang *et al*., 2014), promotes energy expenditure, and reduces body weight, thereby improving nonalcoholic steatohepatitis in HFD-induced obesity mice (Jia *et al*., 2016). Because skeletal muscle is one of the main regulators not only of carbohydrate but lipid metabolism. This study aims to identify the efficacy of LBP in in preserving skeletal muscle mass and glucolipid metabolism by activating the PI3K/AKT signaling pathway, thus providing a scientific foundation for the traditional "muscle-strengthening" function of *L. barbarum* and offering insights into potential therapeutic targets and treatment strategies for SO.

MATERIAL AND METHOD

Experimental animals. The animal study was reviewed and approved by the Ethics Committee of Ningxia Medical University, Yinchuan, China (permit number: NYLAC-2022-141).

Five-week-old male C57BL/6J mice were purchased from Beijing Vital River Laboratory Animal Technology Co., Ltd. (Beijing, China) and housed in a specific pathogen-free (SPF) barrier facility at the Animal Centre of Ningxia Medical University (Yinchuan, China). The mice were maintained at a constant temperature (25 ± 1 °C) with a 12 h:12 h light-dark cycle and had free access to food and water. After a 1-week adaptation period, all mice were randomly divided into 2 groups: those fed a normal diet (ND group; 10 % kcal fat; n=12) and those fed a high-fat diet (HFD group; 60 % kcal fat; Jiangsu Xietong Pharmaceutical Bio-engineering, China; n=90) for 17 weeks to induce obesity. Following the evaluation of the mouse models, the HFD group mice were further subdivided into several subgroups (n=10 each): HFD-fed group (SO group), LBP-L group (Bairuiyuan, Ningxia, China) (SO + LBP 50 mg/kg group), LBP-M group (SO + LBP 100 mg/kg group), and LBP-H group (SO + LBP 200 mg/kg group). For the LBP administrated groups, the HFD was continued for 17 weeks, followed by oral administration of LBP for 9 weeks while maintaining HFD. Body weight measurements were taken biweekly to assess food efficiency. At the end of drug administration period, mice were euthanized via cervical dislocation for blood collection. Subsequently, the liver, gastrocnemius (GAS) and mesenteric fat (MAT) were harvested for observation and analysis.

Blood sampling and serum assay. Collected blood samples were centrifuged at 3000 rpm for 15 min at 4 °C. Serums samples were then collected for the measurement of lipid, glucose, and insulin levels. Glucose, aspartate aminotransferase (AST), alanine transaminase (ALT), total cholesterol (TC), triglyceride (TG), high-density lipoprotein (HDL-C), and low-density lipoprotein (LDL-C) levels were determined using an automatic biochemistry analyzer (ADVIA 2400, Simon, Germany). Glucose and insulin levels were quantitatively measured using a glucometer (Sinocare, Changsha, China) and an enzymatic kit (Elabscience, Wuhan, China) respectively. The insulin resistance index (HOMA-IR) was calculated using the following formula: HOMA-IR = fasting glucose (mmol/L) × fasting insulin (mU/L)/22.5.

Histological analysis. Harvested liver and mesenteric fat tissues were fixed in 4 % paraformaldehyde solution for 24 h, embedded in paraffin, and sectioned into 5 μm slices. The sections were stained with hematoxylin and eosin (HE), and images were captured using an optical microscope (Olympus, Tokyo, Japan) at ×100 magnification. Image J software (National Institute of Health, Bethesda, MD, USA) was used to quantify the cross-sectional area (CSA) of approximately 15 to 20 adipocytes and muscle cells per image.

Fresh liver samples were fixed in 4 % paraformaldehyde for 4 h and embedded in optimal cutting temperature (OCT) compound. Frozen sections (8mm) were generated using a cryostat and fixed with 4 % paraformaldehyde for an additional 30 min. The slides were washed with distilled water and stained with Oil Red O for 15 min to determine lipid content in the liver tissue.

Cell culture and treatment. C2C12 myoblast cells (Zhongqiaoxinzhou Biotech, Shanghai, China) were cultured in Dulbecco's Modified Eagle's Medium (DMEM, Zhongqiaoxinzhou Biotech, shanghai, China) supplemented with 4.5 g/L D-glucose, 10 % fetal bovine serum (FBS, Gibco, Carlsbad, CA, USA), 1 % penicillin-streptomycin solution (Gibco, Carlsbad, CA, USA), and 1 % sodium

pyruvate (100Mm; Zhongqiaoxinzhou Biotech, Shanghai, China) in a humidified atmosphere of 5 % CO_2 at 37 °C. For cell differentiation, the medium was replaced with differentiation medium (DMEM supplemented with 2 % horse serum and 1 % penicillin-streptomycin) for 4 days. The resulting myotubes were treated with 0.1 mM palmitic acid (PA, Sigma-Aldrich, St Louis, MO, USA) and 300 mg/mL LBP for 24 h.

Myotube diameter analysis. Following incubation, myotubes were imaged at 20 × magnification using a phase contrast microscope (IX73, Olympus, Tokyo, Japan). The average myotube diameter was measured and quantified using Image J software (Scion, Frederick, MD, USA).

Glucose uptake assay. C2C12 myotubes were incubated in glucose-free DMEM containing 100mM of 2-deoxy-2-[(7-nitro-2,1,3-benzoxadiazol-4-yl) amino]-D-glucose (2-NBDG, MCE, USA) for 30 min at 37 °C under a humidified atmosphere of 5 % CO_2. After incubation, glucose uptake was evaluated using a fluorescence microscope (BX51, Olympus, Tokyo, Japan). The glucose uptake was quantified by measuring the fluorescence intensity through Image J software.

Muscle triglycerides analysis. The preparation of GAS or myotubes samples and the measurement of triglyceride content were performed according to the manufacturer's instructions using a colorimetric triglyceride assay kit (Elabscience, Wuhan, China). The absorbance of the samples was measured at 510 nm using a SpectraMax Paradigm plate reader (Molecular Devices). The protein concentration of muscle and cell homogenates was determined to calculate the TG content in muscle and cells.

Western blot assay. Gastrocnemius muscle tissues and C2C12 myotubes were lysed in cold RIPA buffer (Solarbio, Beijing, China) containing a mixture of protease and phosphatase inhibitors (Solarbio, Beijing, China). Protein quantification was performed using a bicinchoninic acid protein assay kit (Thermo Fisher Scientific, Waltham, MA, USA). Protein samples were subjected to SDS-PAGE and transferred to polyvinylidene fluoride membranes. The membranes were incubated with the corresponding primary antibodies, including anti-phosphorylated (p)-PI3K (Thr172, 1:1000, Cell Signaling Technology, Danvers, MA, USA), anti-PI3K (1:1000, CST), anti-p-AKT (1:1000, CST), anti-AKT (1:1000, Abcam, Cambridge, UK), anti-p-FOXO-3a (1:1000, CST), anti-FOXO-3a (1:1000, CST), anti-Atrogin-1 (1:1000, Abcam), anti MuRF-1 (1:1000, Proteintech, Wuhan, China), anti-myostatin (1:1000, Proteintech), anti-ActRIIβ (1:1000, Proteintech), anti-IRS-1 (1:1000, Proteintech), anti-mTOR (1:1000, Abcam), anti-p-mTOR (1:1000, CST), anti-GLUT-4 (1:2000, Proteintech), anti-P70S6K (1:1000, CST), anti-GSK3β (1:1000, Proteintech), anti-eIF2B (1:1000, Proteintech), anti-p-Smad2/3 (1:1000, CST), anti-Smad2/3 (1:1000, CST) and anti-GAPDH (1:5000, Proteintech) overnight at 4 °C. The membranes were then incubated with the secondary antibody for 1 h at 37 °C. The protein bands were visualized using a C600 luminescent image analyzer (Fujifilm, Tokyo, Japan) with an enhanced chemiluminescent detection reagent (Thermo Fisher Scientific, Waltham, MA, USA). The visualized protein bands were normalized to GAPDH and quantified using Image J software.

Statistical analysis. Data were expressed as mean ± standard deviation (SD). Statistical analysis was performed using GraphPad Prism 9.4.0 software, and conducted using a one-way ANOVA and Tukey's test. SPSS version 25 statistical software (Chicago, IL, USA) was used to determine statistical significance, with *P*-values less than 0.05 considered statistically significant and *P*-values less than 0.01 considered highly statistically significant.

RESULTS

LBP suppresses obesity in HFD-induced SO mice. As shown in Fig. 1, mice fed an HFD exhibited significantly higher body weight compared to those in the ND group. However, the body weight decreased in a dose-dependent manner in the LBP administration groups (e.g. body weight was significantly decreased by about 10.64 % in the L-H group compared to the SO group.) (Fig. 1a and c). Additionally, LBP treatment significantly reduced the weight of mesenteric fat and the CSA of adipocytes in a similar dose-dependent manner (Fig. 1d-f).

Moreover, HE and oil red O staining of liver tissues revealed that LBP administration improved hepatocyte steatosis and lipid droplet deposition compared to the SO group (Fig. 1g). Furthermore, LBP treatment alleviated HFD-induced liver weight gain (Fig. 1h). Serum levels of AST and ALT were significantly elevated in SO mice compared to the ND group, but LBP treatment attenuated these increases (Fig. 1i and j).

LBP prevents muscle atrophy in HFD-induced SO mice. To clarify whether LBP administration retarded muscle atrophy in obesity-induced mice, we measured the gastrocnemius mass, muscle fiber CSA, and protein level of muscle atrophy factors to determine muscular improvement. The result showed that the wet weight of GAS and the muscle-to-body weight ratio in LBP-H group was significantly increased compared to the SO group (Fig. 2a and b). HE staining revealed that LBP administration ameliorated the damaged myofiber architecture and

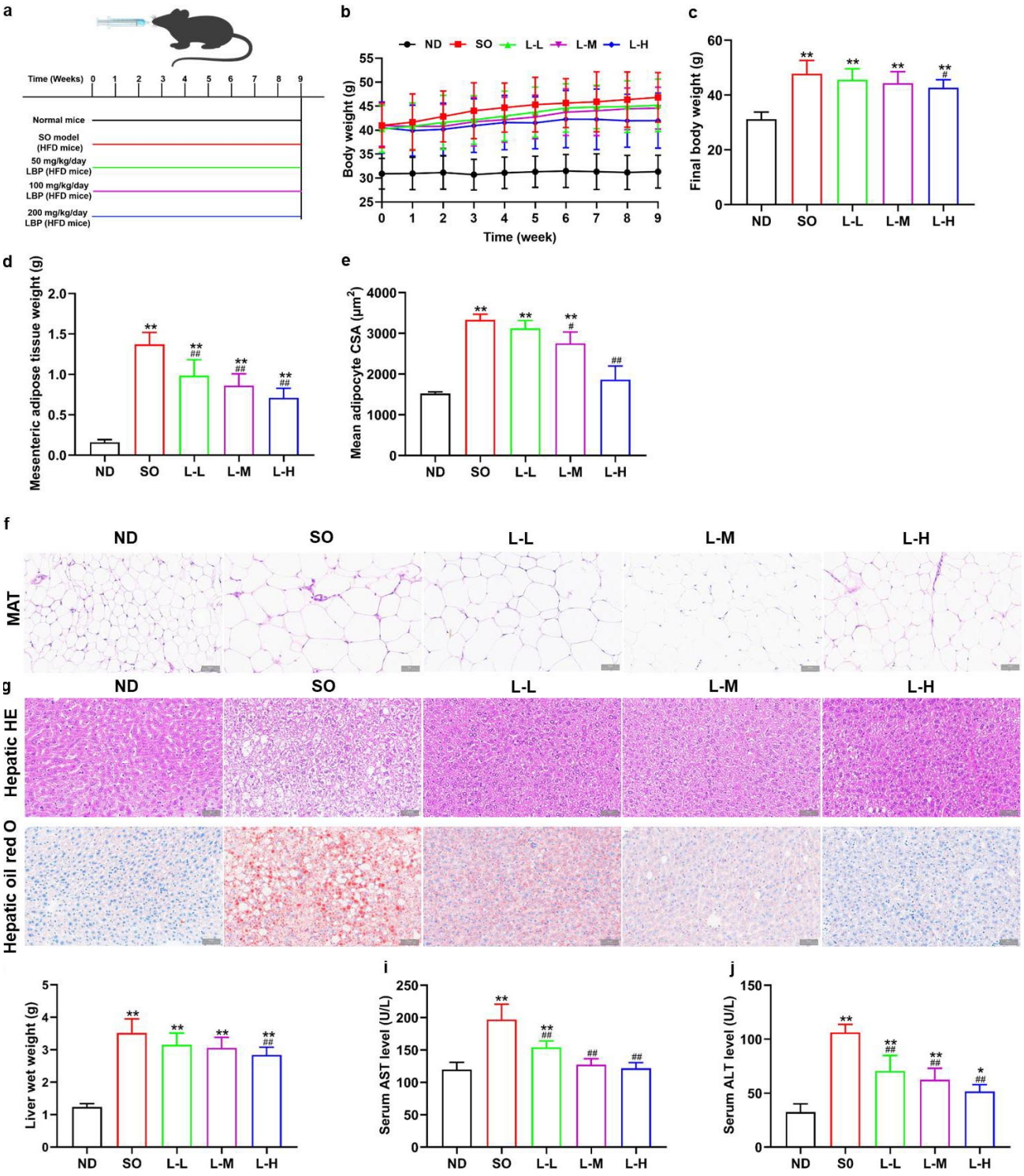

Fig. 1. LBP regulated obesity in HFD-induced SO mice. (a) Schematic diagram of LBP treatment. (b, c) Average body weight curves and changes in body weight after LBP treatment, n = 8. (d) The weight of mesenteric fat. (e) The mean cross-sectional area (CSA) of adipocyte in mesenteric fat. (f) Representative HE staining of mesenteric fat. Scale bars 50 μm, n = 3. (g) Representative HE and oil red O staining of liver sections. Scale bars 50 μm, n = 3. (h) The weight of liver, n = 8. (i, j) AST, ALT concentration in the liver. The data are shown as mean ± SD. **P* < 0.05, ***P* < 0.01 compared with the ND group, #*P* < 0.05, ##*P* < 0.01 compared with the SO group. n = 6.

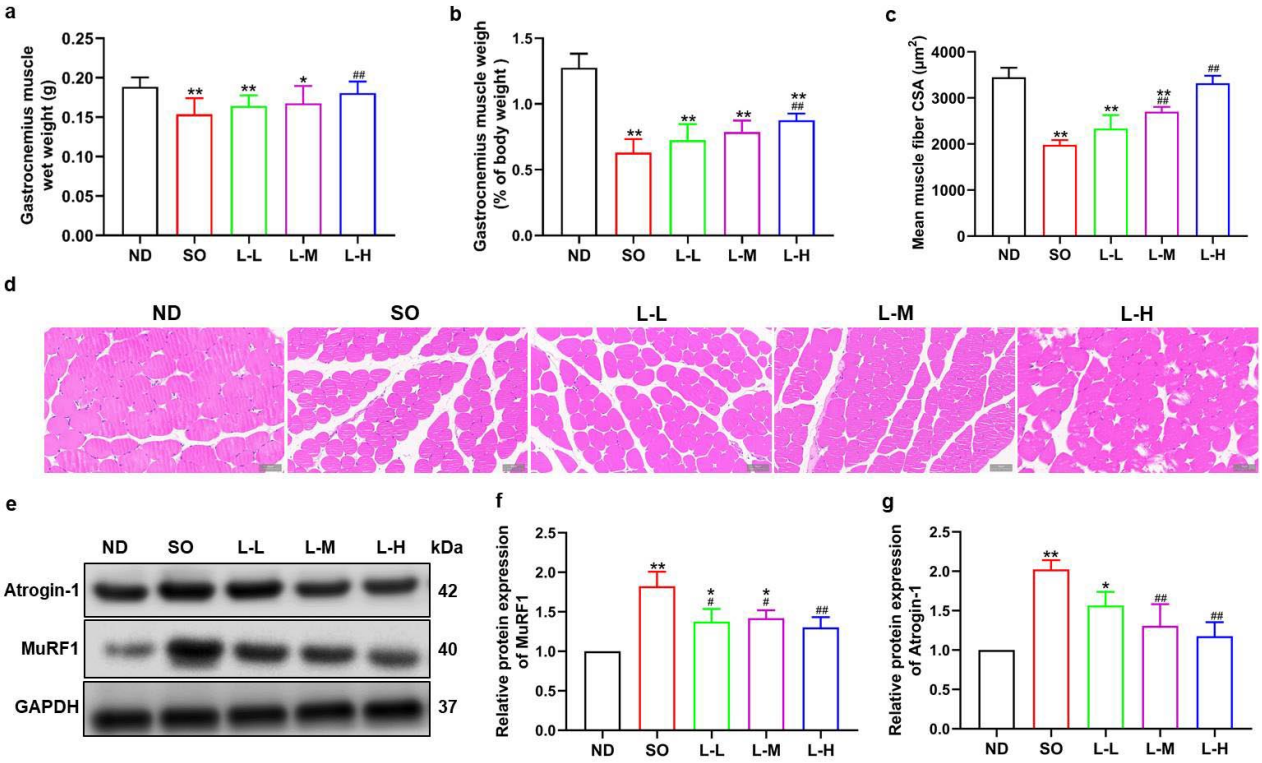

Fig. 2. LBP protected against skeletal muscle atrophy in HFD-induced SO mice. (a) The wet weight of gastrocnemius (GAS), n = 12. (b) The ratio of GAS weight to body weight (mg/g), n = 12. (c) The mean muscle fiber CSA of GAS, n = 3. (d) Representative HE staining of GAS. Scale bar 50 μm, n = 3. (e-g) Representative western blot images and relative protein expression levels of Atrogin-1 and MuRF1 in GAS. The data are shown as mean ± SD. **P* < 0.05, ***P* < 0.01 compared with the ND group, #*P* < 0.05, ##*P* < 0.01 compared with the SO group. n = 6.

decreased the mean fiber CSA in SO mice (Fig. 2c and d). Furthermore, Atrogin-1 and MuRF1 protein levels significantly increased in the HFD-induced SO mice, however, LBP administration significantly decreased the protein levels of these factors, compared with the SO mice (Fig. 2e-g). These results implied that LBP effectively ameliorated HFD-induced skeletal muscle atrophy.

LBP ameliorates insulin resistance, dyslipidemia, and muscle lipotoxicity in HFD-induced SO mice. We investigated the effect of LBP on insulin resistance, both fasting blood glucose and insulin levels decreased significantly in the LBP administration compared to the SO group. By calculating HOMA-IR, we confirmed that insulin resistance was improved in LBP administration groups in a dose-dependent manner (Fig. 3a-c). Furthermore, excess lipid is stored as lipid drops in gastrocnemius muscle ectopically, which causes insulin resistance. The concentration of intramyocellular triglyceride was significantly increased in the SO group and significantly reduced by LBP administration (Fig. 3d). Serum TC, TG and LDL-C levels were significantly decreased by LBP administration and HDL-C level tended to increase by LBP administration (Fig. 3e-h). Furthermore, compared with ND group, the protein levels of IR, IRS-1, p-PI3K/PI3K, p-AKT/AKT and GLUT-4 in SO group decreased, while the above protein expressions increased after LBP intervention and is better in LBP-H (Fig. 3i-n). Thus, LBP administration alleviated obesity induced insulin resistance, dyslipidemia, and skeletal muscle lipotoxicity effectively via PI3K/AKT pathway.

LBP improves obesity-induced muscle atrophy via the PI3K/AKT pathway in SO mice. When PI3K/AKT signaling pathway is activated, muscle protein synthesis is increased by factors of mTOR/p70S6K and GSK3β/eIF2B. Therefore, we investigated the effect of LBP on the protein synthesis factors. The protein levels of p-mTOR/ mTOR and p70S6K were significantly decreased in the SO group compared to the ND group, however, these indexes were increased in LBP administration groups in a dose-dependent manner, and were restored to the normal level in the L-H group (Fig.

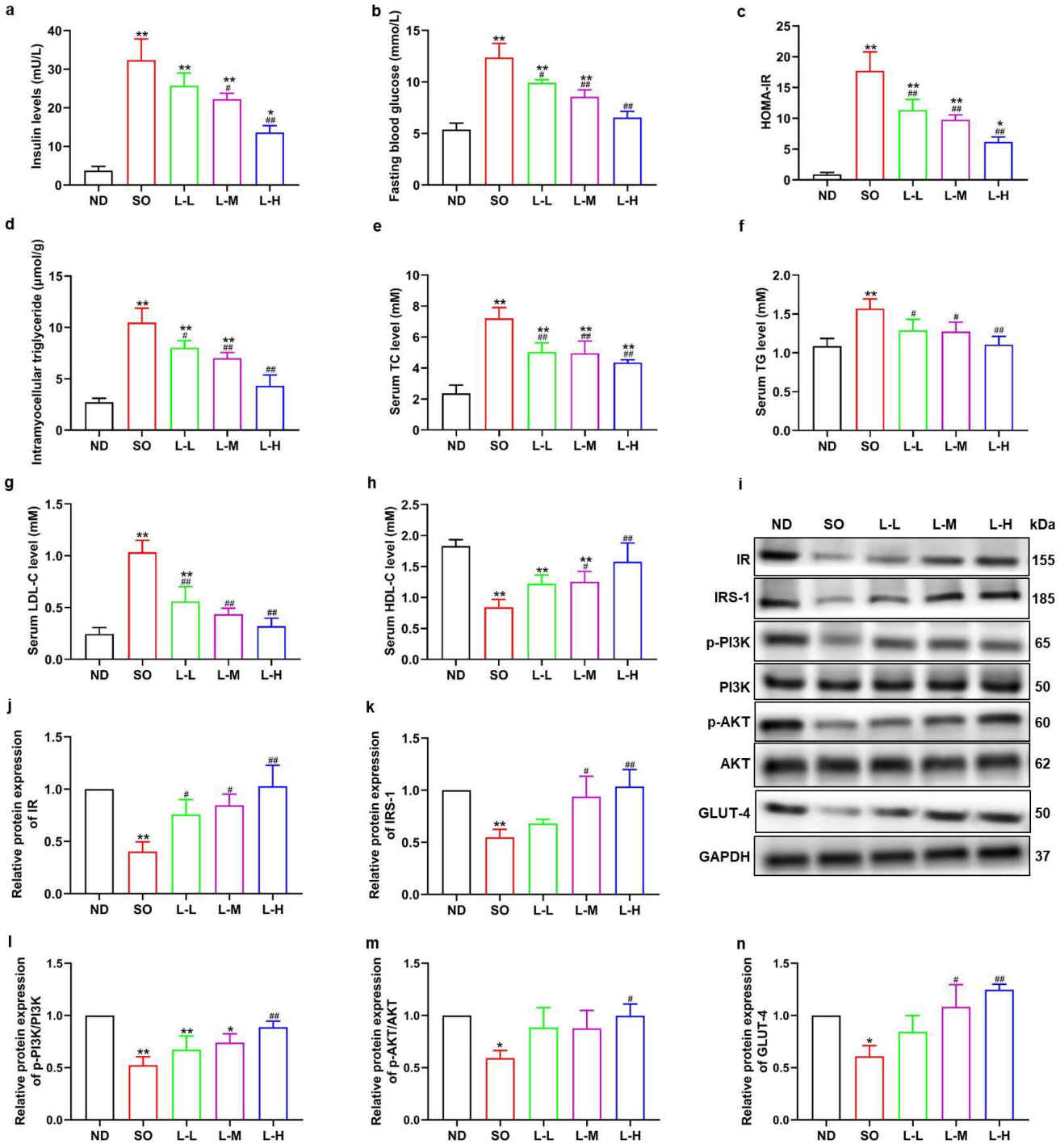

Fig. 3. LBP regulated glucose and lipid metabolism in HFD-induced SO mice. (a) Fasting blood glucose levels, n = 3. (b) Fasting blood insulin levels, n = 3. (c) Homeostasis model assessment of insulin resistance (HOMA-IR) index, n = 3. (d) Total triglyceride concentration in the gastrocnemius muscle tissue, n = 3. (e-h) Serum total TC, TG, LDL-C, HDL-C concentration, n = 4. (i-n) Western blot images and relative protein expression levels of factors related to insulin signaling pathway. The data are shown as mean ± SD. **P* < 0.05, ***P* < 0.01 compared with the ND group, #*P* < 0.05, ##*P* < 0.01 compared with the SO group. n = 6.

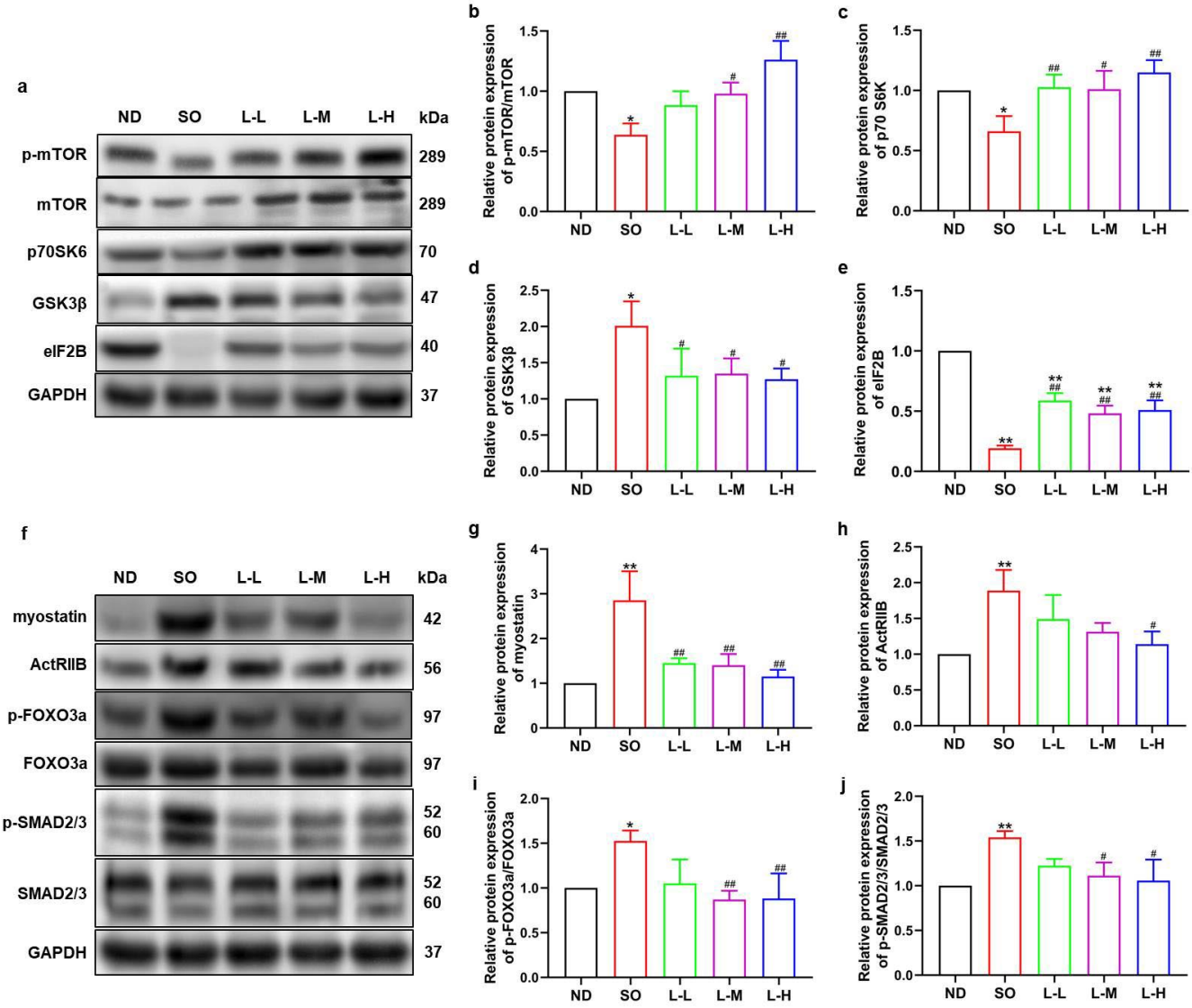

Fig. 4. Effect of LBP on muscle protein synthesis and degradation via PI3K/AKT pathway in HFD-induced SO mice. (a) Western blot images of factors related to muscle protein synthesis in gastrocnemius. (b-e) Relative protein expression levels of factors related to muscle protein synthesis in gastrocnemius. (f) Western blot images of factors related to muscle protein degradation in gastrocnemius. (g-j) Relative protein expression levels of factors related to muscle protein degradation in gastrocnemius. The data are shown as mean ± SD. **P* < 0.05, ***P* < 0.01 compared with the ND group, #*P* < 0.05, ##*P* < 0.01 compared with the SO group. n = 6 per group.

4a-c). The protein levels of GSK3b showed a significant increase and eIF2B expression decreased in the SO group compared with the ND group, while LBP administration recovered the expression levels of GSK3β and eIF2B dose dependently (Fig. 4a, d and e).

For muscle protein degradation, the myostatin, and ActRIIβ, p-FOXO3a/FOXO3a, p-SMAD2/3/SMAD2/3 were significantly increased in the SO group compared to the ND group, while LBP administration significantly reduced and recovered to the normal level in the L-H group except for myostatin. Thereby the protein expression of Atrogin-1 and MuRF1 were significantly decreased by LBP administration (Fig. 4f-j).

LBP attenuates PA-induced glucose and lipid metabolism derangement, muscle atrophy in C2C12 myotubes. To investigate the efficacy of LBP against PA-induced muscle atrophy in C2C12 cells, the concentration of 0.1mM PA and 300mg/mL LBP were selected to treat

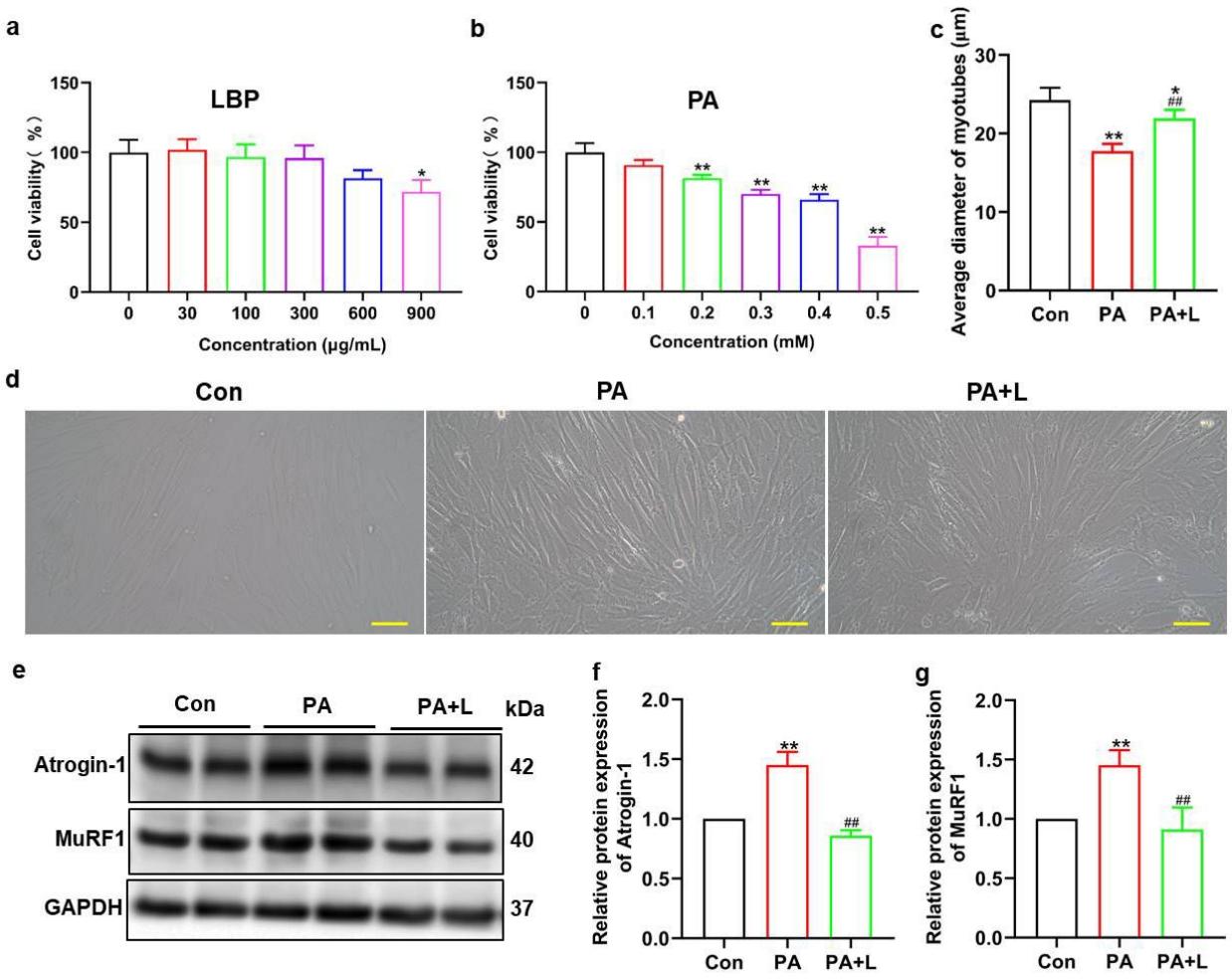

Fig. 5. LBP improved myotube atrophy in PA-induced muscle atrophy C2C12 myotubes. (a, b) Cell viability of C2C12 myoblasts was measured in different concentrations of PA (0, 0.1, 0.2, 0.3, 0.4 and 0.5mM) and LBP (0, 30, 100, 300, 600 and 900 mg/mL). (c, d) 400× magnification images of myotubes and the quantitative of average diameter. Scale bar 50 μm, n = 3. (e-g) Representative western blot images and relative protein expression levels of Atrogin-1 and MuRF1 in myotubes. The data are shown as mean ± SD. **P* < 0.05, ***P* < 0.01 compared with the Con group, #*P* < 0.05, ##*P* < 0.01 compared with the PA group. n = 6.

cells based on the cell viability (Fig. 5a and b). Myotube diameter was significantly reduced in the PA treated group, indicating that muscle atrophy was induced by PA and it was significantly recovered by LBP treatment (Fig. 5c and d). The protein expression levels of Atrogin-1 and MuRF1 markedly decreased after LBP administration relative to those of PA group (Fig. 5e-g).

Moreover, we identified whether LBP was involved in regulating PA-induced glucose and lipid metabolic derangement. 2-NBDG uptake assay and intracellular TG content were performed to confirm impaired glucose uptake and lipid accumulation in the PA-induced myotubes compared to the control group, but LBP intervention significantly inhibited this phenomenon (Fig. 6a-c). Western blot results showed that LBP intervention significantly increased the protein expression of the IR, IRS-1, p-PI3K/PI3K, p-AKT/AKT and GLUT-4 compared with PA group (Fig. 6d-i). These results suggested that LBP improved PA-induced glucose and lipid disturbance, in C2C12 myotubes.

For muscle protein synthesis and degradation, the results showed that PA intervention could inhibit the synthesis and promote the degradation of protein, that is, PA intervention could lead to the imbalance between the synthesis and degradation resulting in the atrophy. However, LBP administration can restore the homeostasis of protein metabolism and inhibit the muscle atrophy in PA-induced myotubes (Fig. 7a-j).

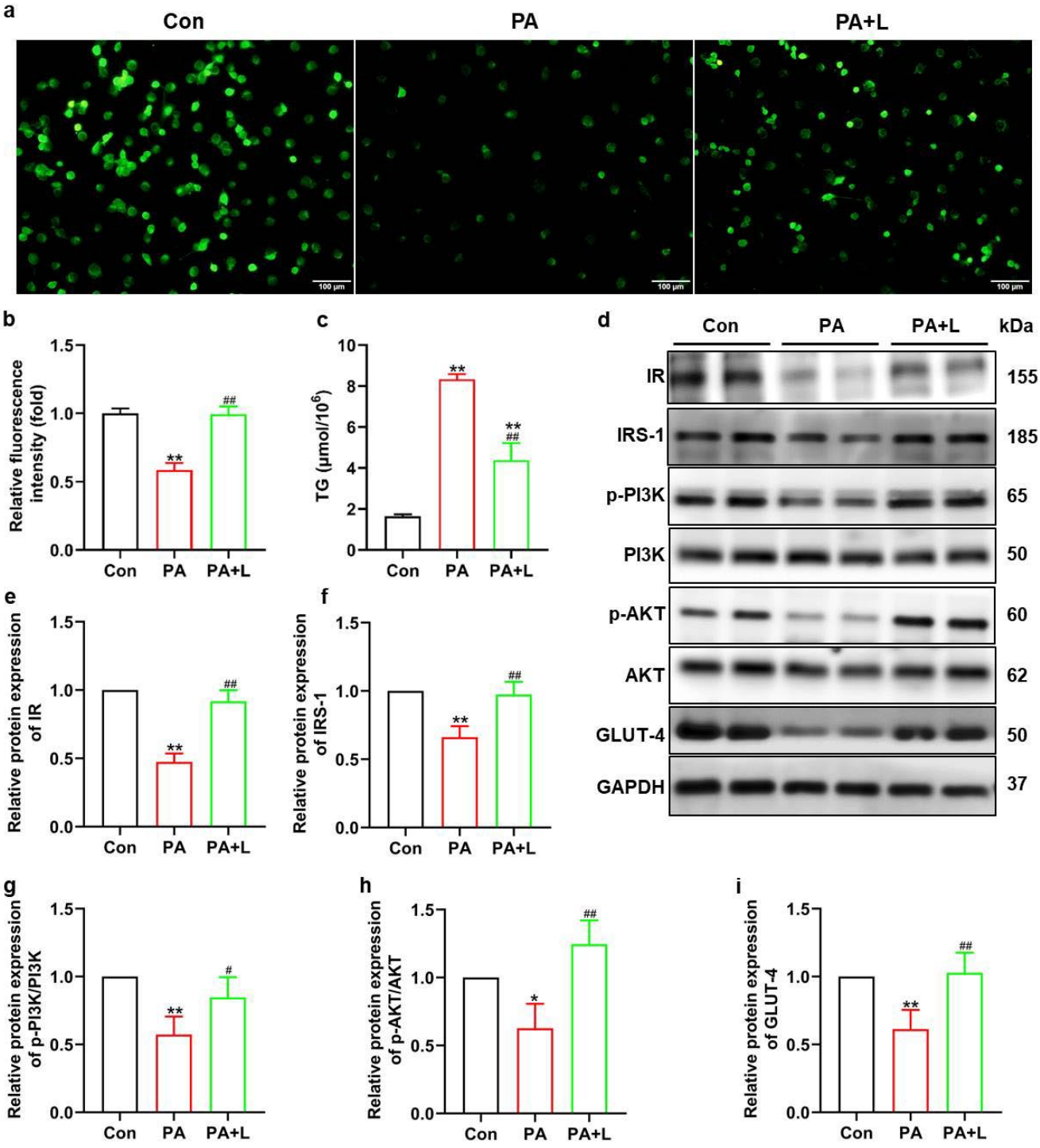

Fig. 6. LBP improved lipid and glucose metabolism disorder in PA-induced muscle atrophy C2C12 myotubes. (a, b) Representative images and quantitative graph of glucose uptake in myotubes. Scale bar 50mm, n = 3. (c) Changes of TG levels in myotubes, n = 4. (d-i) Western blot images and relative protein expression levels of IR, IRS-1 p-PI3K/PI3K, p-AKT/AKT and GLUT-4 in myotubes. The data are shown as mean ± SD. *P < 0.05, **P < 0.01 compared with the Con group, #P < 0.05, ##P < 0.01 compared with the PA group. n = 6.

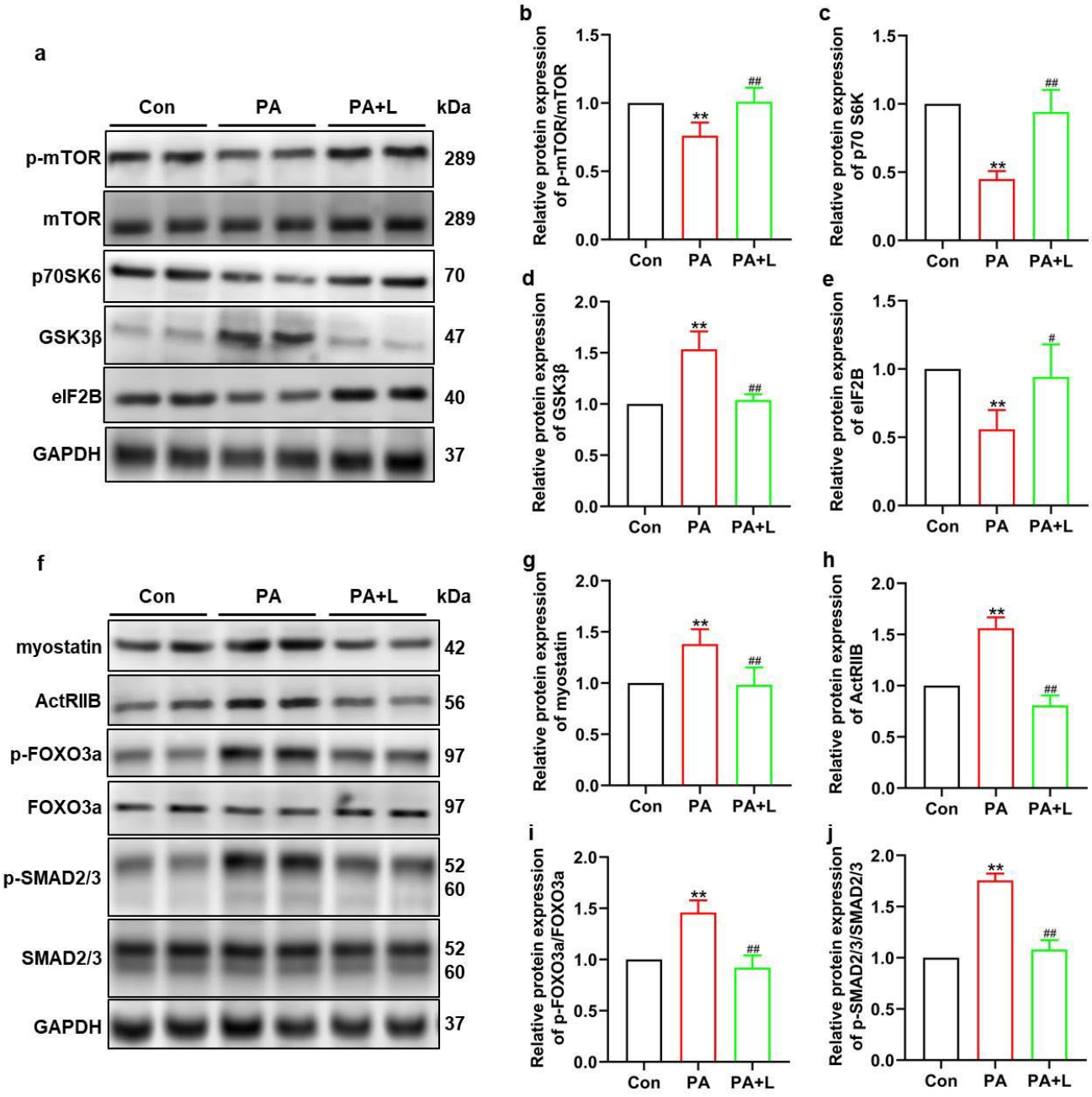

Fig. 7. LBP improved muscle protein synthesis and degradation via PI3K/AKT pathway in PA-induced muscle atrophy C2C12 myotubes. (a) Western blot images of factors related to muscle protein synthesis in C2C12 myotubes. (b-e) Relative protein expression levels of factors related to muscle protein synthesis in C2C12 myotubes. (f) Western blot images of factors related to muscle protein degradation in C2C12 myotubes. (g-j) Relative protein expression levels of factors related to muscle protein degradation in C2C12 myotubes. The data are shown as mean ± SD. **P* < 0.05, ***P* < 0.01 compared with the Con group, #*P* < 0.05, ##*P* < 0.01 compared with the PA group. n = 6 per group.

DISCUSSION

This study demonstrated the remarkable protective effects of LBP on high-fat-diet (HFD) induced sarcopenia. Results showed that LBP administration could mitigate obesity, glucolipid metabolism, balance of skeletal muscle protein synthesis and degradation in SO mice via activating the PI3K/AKT signaling pathway, indicating that LBP may

be a potential therapeutic agent to prevent muscle atrophy caused by long-term HFD feeding in mice.

Obesity is primarily caused by the consumption of an unhealthy diet with a prolonged imbalance of energy intake and energy expenditure, accompanied by excessive accumulation of fat in visceral adipose tissue and ectopic fat deposition in liver, heart and skeletal muscle (Alalwan, 2020). It is well-known that HFD induces obesity in animals. In this study, we observed a marked increase in body weight, mesenteric fat mass and adipocyte CSA after 17 weeks of HFD feeding in SO mice. Additionally, mice fed an HFD exhibited typical characteristics of fatty liver. Previous study reported that visceral adipose tissue (but not subcutaneous) influences systemic insulin metabolism by releasing free fatty acids (FFAs) (Dhokte & Czaja, 2024), which continue to induce insulin resistance in other tissues as FFAs are released into plasma from adipose tissue and transported to other sites like the liver via the portal vein and to skeletal muscle through its vasculature (Sears & Perry, 2015). Especially mesenteric fat, which is drained by the portal circulation, is metabolically active tissue. The mesentery stores most of the intra-abdominal fat, and has emerged as a key contributor to insulin resistance and diabetes via recruitment of inflammatory cells and the secretion of adipokines, cytokines, free fatty acids, and other diabetogenic factors. Therefore, it plays an important role in dyslipidemia and visceral obesity through increased FA and cytokine production (Liu *et al*., 2006). Previous study reported that mesenteric fat reduction using a tissue liquidation technique on insulin resistant non-human primates served to improve insulin sensitivity and reduce body weight (Andrew *et al*., 2018). Comfortingly, LBP effectively and significantly reduced mesenteric fat mass and CSA of adipocytes. LBP has demonstrated efficacy in alleviating obesity by reducing lipid droplet accumulation in obese mice (Zhou *et al*., 2024), and improving hepatic lipid metabolism via the SIRT1/AMPK pathway (Jia *et al*., 2016). Therefore, LBP effectively and significantly reduced the body weight, fat mass, adipocyte CSA and alleviating fatty liver, thereby alleviating obesity induced by HFD.

Metabolically healthy skeletal muscles store both glucose and FFAs as a source of energy. However, when there is an excess of FFAs in the bloodstream, skeletal muscle will uptake more of them, which may lead to an accumulation within muscle fibers (Abdul-Ghani & DeFronzo, 2010). When broken down, these stored fats are converted to metabolites such as long-chain acyl-CoAs, ceramides, and diacylglycerols, excess accumulation of these lipid intermediates in skeletal muscle has been shown to inhibit insulin signaling activities, resulting to suppression of insulin-stimulated glucose transport in the cytosol (Abdul-Ghani & DeFronzo, 2010). In practice, as mesenteric fat decreased following LBP administration, we observed alleviation of the serum lipid profile and insulin resistance in this study. Skeletal muscle is the primary and largest site for modulating normal glucose concentrations in the postprandial state in humans. More than 80 % of glucose uptake activity is regulated in skeletal muscle under euglycemic hyperinsulinemic conditions (Abu-Bakar & Tan, 2017; Mok *et al*., 2021). In skeletal muscle, insulin binds to its receptor, leading to activation of PI3K, which subsequently activates AKT at the plasma membrane. This process is essential for GLUT-4 translocation and subsequent glucose uptake into skeletal muscle (Tang *et al*., 2017; Mok *et al*., 2021). IRS-1/PI3K/AKT/GLUT-4 signaling pathway are considered to maintain glucose homeostasis and insulin sensitivity. Our study showed that LBP intervention significantly increased the protein expression of these molecules and enhanced glucose uptake. Consequently, LBP supplementation improved insulin resistance through upregulating IRS-1, activating PI3K/AKT, facilitating GLUT-4 translocation. In obesity, excess fatty acids are stored as triacylglycerols within lipid droplets in skeletal muscle, disrupting the PI3K/AKT pathway and exacerbating insulin resistance (Ferretti *et al*., 2018; Han & Choung, 2022). Our results showed that LBP administration inhibited ectopic lipid accumulation in muscle fibers and liver. Additionally, AST and ALT are biomarkers of liver injury. LBP administration significantly reduced the concentrations of AST and ALT in the liver in this study. In our previous research, we showed that LBP markedly reduced the liver weight and TG levels in the serum and liver of HFD-induced mice (Jia *et al*., 2016). A cohort study involving 13,692 individuals demonstrated that coexistence of metabolic-associated fatty liver disease and sarcopenia further increases mortality risk (Zhao *et al*., 2023). Therefore, protecting against liver damage may be beneficial for preventing sarcopenia. As expected, LBP is effective in reducing metabolic syndrome by decreasing ectopic fat deposition and improving glucose and lipid metabolism disorders.

Sarcopenia and insulin resistance (IR) are closely linked. In compensatory hyperinsulinemia due to IR, glycogenesis is poorly suppressed, protein degradation is accelerated, and protein synthesis is reduced (Nishikawa *et al*., 2021), leading to increased myostatin levels that contribute to skeletal muscle loss (Baczek *et al*., 2020). Skeletal muscle fiber atrophy is a major pathological feature observed in sarcopenia. The PI3K/AKT pathway plays a crucial role in maintaining metabolic homeostasis in obesity and obesity-related complications. It is a key mediator of

insulin signaling in muscles, stimulating protein synthesis via mTOR and suppressing protein degradation via FoxO3a (Ueda-Wakagi *et al*., 2018). Consistent with this, our study showed that the protein levels of p-PI3K/PI3K and p-AKT/AKT in SO group significant decreased, indicating inactivated of the PI3K/AKT pathway exacerbates muscle atrophy. Mammalian target of rapamycin (mTOR) is a downstream target of AKT, and mTOR activity is highly correlated with the anabolic/catabolic balance. The IGF-1/PI3K/AKT/mTOR pathway has been shown to be indispensable in promoting muscle hypertrophy (Sartori *et al*., 2021). p70S6K, a downstream target of mTOR, is an enzyme that targets the S6 ribosomal protein and stimulates protein synthesis. Our results showed that LBP administration significantly increased the expression of these proteins in a dose-dependent manner. Additionally, AKT promotes protein synthesis by inhibiting the expression of glycogen synthase kinase 3β (GSK3β). Consequently, inhibition of GSK3β increases the expression of eukaryotic initiation factor 2B (eIF2B), leading to enhanced protein synthesis. LBP inhibited GSK3β expression and increased eIF2B expression, thereby promoting protein synthesis. In this study, we found that gastrocnemius mass and muscle fiber CSA were significantly restored in the LBP-H group. Therefore, these findings indicate that LBP administration significantly mitigated HFD-induced inhibited the protein synthesis by through the PI3K/AKT in obese mice.

Maintenance of muscle mass also depends on protein-degrading metabolism. As a downstream member of the PI3K/AKT signaling pathway, FoxO3a holds a leading position in protein degradation within the musculoskeletal system. The resulting target gene is the ubiquitin ligase Atrogin-1 and MuRF1, which causes skeletal muscle atrophy (Gellhaus *et al*., 2023). Wang *et al*. (2021), reported that inhibition of PI3K/AKT phosphorylation promotes muscle atrophy by FoxO3a-mediated transcriptional activation of Atrogin1 and MuRF1. Myostatin is known as a negative regulator of myogenesis and is produced mainly by skeletal muscle, which can induce the downstream targets of ActRIIβ and SMAD2/3 stimulating the ubiquitin-proteasome pathway and leading to the muscle atrophy (Lee *et al*., 2019). Our study showed that HFD induced an increase in the expression of p-FoxO3a/FoxO3a ratio, myostatin, p-SMAD2/3/SMAD2/3 ratios and ActRIIB in skeletal muscle, while LBP administration can decrease those protein levels so that Atrogin-1 and MuRF1 expression were decreased and inhibit protein degradation, and attenuated muscle atrophy. Indeed, recent studies have confirmed that increased muscle mass correlates with decreased expression of Atrogin1 and MuRF1 (Han & Choung, 2022; Shin *et al*., 2020). To sum up, disrupted PI3K/AKT pathway induced by obesity exacerbating systemic insulin resistance and the development of muscle atrophy. However, the imbalance between protein synthesis and degradation was restored through improved insulin signaling by LBP administration, leading to recovered muscle mass.

In summary, LBP can effectively ameliorate obesity and muscle atrophy. These effects are attributed to its ability to modulate glucolipid metabolism and alleviate insulin resistance in skeletal muscle via the PI3K/AKT pathway, as well as activate protein synthesis and inhibit protein degradation in HFD-induced obese mice.

CONCLUSION

In conclusion, the findings of this study demonstrate that LBP can effectively modulate glucolipid metabolism and restore the balance between protein synthesis and degradation, thereby improving skeletal muscle atrophy through activation of the PI3K/AKT pathway in HFD-induced obese mice. These results provide experimental evidence supporting the potential application of LBP in treating obesity-related conditions and offer a scientific basis for the traditional "muscle-strengthening" function of *L. barbarum*. However, it is important to acknowledge certain limitations within this research. Further investigation into the molecular mechanisms underlying LBP's protective effects is necessary to fully elucidate these processes and explore their potential in greater depth.

GONG, F.; REN, Y.; CAO, T.; XU, Y.; WANG, K.; LI, J.; JIN, Z.; WANG, A.; LI, J.; YANG, Y. & WEI, Y. El polisacárido de *Lycium barbarum* mejora la atrofia muscular inducida por la obesidad mediante la activación de la vía PI3K/AKT. *Int. J. Morphol., 43(4)*:2001-2014, 2025.

RESUMEN: La acumulación anormal o excesiva de grasa causada por un estilo de vida sedentario y una dieta rica en grasas (HFD) puede provocar pérdida de masa y fuerza muscular, lo que finalmente resulta en sarcopenia, una afección conocida como obesidad sarcopénica (OS). Este estudio tuvo como objetivo investigar los efectos del polisacárido de *Lycium barbarum* (LBP) sobre la OS y explorar los mecanismos subyacentes para evaluar su potencial como agente terapéutico natural. Ratones machos C57BL/6J fueron alimentados con una dieta alta en grasas (HFD) durante 17 semanas, comenzando la administración de LBP a las 8 semanas y continuando durante 9 semanas. El peso corporal se midió dos veces por semana. Tras la eutanasia, se realizó un análisis histológico de las fibras musculares, un perfil lipídico en sangre, una extracción de triglicéridos musculares y un análisis de transferencia Western. *In vitro*, los mioblastos C2C12 confluentes se diferenciaron durante 4 días y posteriormente se cotrataron con LBP y ácido palmítico (PA) durante 24 horas. Nuestros resultados demostraron que la administración de LBP redujo significativamente el peso corporal, la masa grasa mesentérica y el área transversal de los adipocitos (CSA). Simultáneamente, LBP

aumentó el peso muscular y el CSA de las fibras musculares, a la vez que disminuyó la expresión de marcadores relacionados con la atrofia, como la proteína F-box de atrofia muscular (Atrogin-1) y la proteína RING-finger muscular 1 (MuRF1). Además, el LBP mejoró la tolerancia a la glucosa y la sensibilidad a la insulina al modular la vía de señalización de la fosfatidilinositol-3-quinasa (PI3K)/proteína quinasa B (AKT), lo que también mitigó la acumulación excesiva de lípidos y la deposición ectópica de grasa en el músculo esquelético. La activación de la vía PI3K/AKT por el LBP mejoró la síntesis de proteínas musculares mediante el aumento de la fosforilación de la proteína ribosomal S6 quinasa p70 y la inhibición de la glucógeno sintasa quinasa 3b, a la vez que suprimió la degradación de proteínas musculares mediante la regulación negativa de la expresión de Atrogin-1, MuRF1, miostatina, receptor de activina A tipo II B (ActRIIB) y Smad2/3. Estos hallazgos sugieren que el LBP es un agente natural prometedor para la prevención y el tratamiento de la osteoartritis, ejerciendo sus efectos protectores al corregir los trastornos metabólicos de los glucolípidos y restablecer el equilibrio entre la síntesis y la degradación de proteínas en el músculo esquelético mediante la reactivación de la vía PI3K/AKT alterada.

PALABRAS CLAVE: Dieta alta en grasas; Obesidad sarcopénica; Polisacárido de *Lycium barbarum*; Vía PI3K/AKT; Metabolismo de glucolípidos.

REFERENCES

Abdul-Ghani, M. A. & DeFronzo, R. A. Pathogenesis of insulin resistance in skeletal muscle. *J. Biomed. Biotechnol., 2010*:476279, 2010.

Abu-Bakar, M. H. & Tan, J. S. Improvement of mitochondrial function by celastrol in palmitate-treated C2C12 myotubes via activation of PI3K-Akt signaling pathway. *Biomed. Pharmacother., 93*:903-12, 2017.

Alalwan, T. A. Phenotypes of sarcopenic obesity: exploring the effects on peri-muscular fat, the obesity paradox, hormone-related responses and the clinical implications. *Geriatrics (Basel), 5*:8, 2020.

Andrew, M. S.; Huffman, D. M.; Rodriguez-Ayala, E.; Williams, N. N.; Peterson, R. M. & Bastarrachea, R. A. Mesenteric visceral lipectomy using tissue liquefaction technology reverses insulin resistance and causes weight loss in baboons. *Surg. Obes. Relat. Dis., 1(6)4*:833-41, 2018.

Armandi, A.; Rosso, C.; Caviglia, G. P.; Ribaldone, D. G. & Bugianesi, E. The impact of dysmetabolic sarcopenia among insulin sensitive tissues: a narrative review. *Front. Endocrinol. (Lausanne), 12*:716533, 2021.

Baczek, J.; Silkiewicz, M. & Wojszel, Z. B. Myostatin as a biomarker of muscle wasting and other pathologies. *Nutrients, 12(8)*:2401, 2020.

Deshmukh, A. S. Insulin-stimulated glucose uptake in healthy and insulin-resistant skeletal muscle. *Horm. Mol. Biol. Clin. Investig., 26(1)*:13-24, 2016.

Dhokte, S. & Czaja, K. Visceral adipose tissue: the hidden culprit for type 2 diabetes. *Nutrients, 16(7)*:1015, 2024.

Ferretti, R.; Moura, E. G.; Dos-Santos, V. C.; Caldeira, E. J.; Conte, M.; Matsumura, C. Y.; Pertille, A. & Mosqueira, M. High-fat diet suppresses the positive effect of creatine supplementation on skeletal muscle function by reducing protein expression of the IGF-PI3K-AKT-mTOR pathway. *PLoS One, 13(10)*:e0199728, 2018.

Gellhaus, B.; Böker, K. O.; Schilling, A. F. & Saul, D. Therapeutic consequences of targeting the IGF-1/PI3K/AKT/FOXO3 axis in sarcopenia: a narrative review. *Cells, 12(24)*:2787, 2023.

Han, M. J. & Choung, S. Y. Codonopsis lanceolata ameliorates sarcopenic obesity via recovery of PI3K/Akt signaling and lipid metabolism. *Phytomedicine, 96*:153877, 2022.

Jayaraman, S.; Krishnamoorthy, K.; Prasad, M.; Veeraraghavan, V. P.; Krishnamoorthy, R.; Alshuniaber, M. A.; Gatasheh, M. K. & Gunassekaran. Glyphosate potentiates insulin resistance in skeletal muscle through modulation of IRS-1/PI3K/Akt signaling: an *in vivo* and in silico analysis. *Int. J. Biol. Macromol., 242(Pt. 2)*:124917, 2023.

Jia, L.; Li, W.; Li, J.; Li, Y.; Song, H.; Luan, Y.; Qi, H.; Ma, L.; Lu, X. & Yang, Y. *Lycium barbarum* polysaccharide attenuates high-fat diet-induced hepatic steatosis by up-regulating SIRT1 expression and deacetylase activity. *Sci. Rep., 6*:36209, 2016.

Sears, B. & Perry, M. The role of fatty acids in insulin resistance. *Lipids Health Dis., 14*:121, 2015.

Shin, J. E.; Park, S. J.; Ahn, S. I. & Choung, S. Y. Soluble whey protein hydrolysate ameliorates muscle atrophy induced by immobilization via regulation of the PI3K/Akt pathway in C57BL/6 mice. *Nutrients, 12(11)*:3362, 2020.

Tang, D.; Chen, Q. B.; Xin, X. L. & Aisa, H. A. Anti-diabetic effect of three new norditerpenoid alkaloids via PI3K/Akt signaling pathway modulation. *Biomed. Pharmacother., 87*:145-52, 2017.

Ueda-Wakagi, M.; Hayashibara, K.; Nagano, T.; Ikeda, M.; Yuan, S.; Ueda, S.; Shirai, Y.; Yoshida, K. I. & Ashida, H. Epigallocatechin gallate induces GLUT4 translocation in skeletal muscle through both PI3K- and AMPK-dependent pathways. *Food Funct., 9(8)*:4223-33, 2018.

Wang, L.; Jiao, X. F.; Wu, C.; Li, X. Q.; Sun, H. X.; Shen, X. Y.; Zhang, K. Z.; Zhao, C.; Liu, L.; Wang, M.; *et al*. Trimetazidine attenuates dexamethasone-induced muscle atrophy via inhibition of NLRP3/GSDMD-mediated pyroptosis. *Cell Death Discov., 7(1)*:251, 2021.

Wei, S.; Nguyen, T. T.; Zhang, Y.; Ryu, D. & Gariani, K. Sarcopenic obesity: epidemiology, pathophysiology, cardiovascular disease, mortality, and management. *Front. Endocrinol. (Lausanne), 14*:1185221, 2023.

Yoshida, T. & Delafontaine, P. Mechanisms of IGF-1-mediated regulation of skeletal muscle hypertrophy and atrophy. *Cells, 9(9)*:1970, 2020.

Yang, Y.; Li, W.; Li, Y.; Wang, Q.; Gao, L. & Zhao, J. Dietary *Lycium barbarum* polysaccharide induces Nrf2/ARE pathway and ameliorates insulin resistance via activation of PI3K/Akt signaling. *Oxid. Med. Cell. Longev., 2014*:145641, 2014.

Zhao, Q.; Yin, Y. & Deng, Y. Metabolic-associated fatty liver disease and sarcopenia increase mortality risk: a population-based study. *Nutr. Diabetes, 13(1)*:21, 2023.

Zhou, R.; Liu, Y.; Hu, W.; Yang, J.; Lin, B.; Zhang, Z.; Chen, M.; Yi, J. & Zhu, C. *Lycium barbarum* polysaccharide ameliorates lipid accumulation in adipose tissue via ATF6/SIRT1 signaling. *Acta Biochim. Biophys. Sin. (Shanghai), 56(6)*:844-56, 2024.

Corresponding author:
Yanhong Wei
Ningxia Regional Key Laboratory of Integrated Traditional Chinese and Western Medicine for Prevention and Treatment of Regional High Incidence Disease
Ningxia Medical University
Yinchuan
CHINA

E-mail: lovely_yhwei@126.com

Corresponding author:
Yi Yang
Ningxia Regional Key Laboratory of Integrated Traditional Chinese and Western Medicine for Prevention and Treatment of Regional High Incidence Disease
Ningxia Medical University
Yinchuan
CHINA

E-mail: yangyi73422@163.com